

Delta Journal of Science

Available online at
<https://djs.journals.ekb.eg/>



Research Article

PHYSICS

Morphological, Infrared and Structural Studies for Nano Cobalt Ferrite Doped with Lanthanum

*B.I.SALEM, **O.M.HEMEDA, ***S.F.MANSOUR

* *Department of Physics, Fac. of Science, Tanta University, Tanta, Egypt*

** *Department of Physics, Fac. of Science, Tanta University, Tanta, Egypt*

*** *Department of Physics, Fac. of Science, Zagazig University, Zagazig, Egypt*

Abstract: A series of $\text{La}_x\text{CoFe}_{2-x}\text{O}_4$ prepared by flash method, where $x=0.05, 0.1, 0.15, 0.2, 0.25$ and 0.3 . The powder samples were characterized by X-ray diffraction, FTIR and TEM (transmission Electron Microscope). The x-ray analysis shows that the samples have a single phase cubic spinel structure. The lattice constant was founded to be nearly constant up to $x=0.25$ and then increase as lanthanum content increase. The FTIR spectra of the sample were recorded from $200\text{-}4000\text{ cm}^{-1}$, which analyzed the molecular structure of the samples and the formation of spinel structure in bulk and nano modes. The HRTEM photographs clearly show the presence of cubic nanoparticle with average diameter of 16nm for flash samples. The high resolution (HRTEM) indicates the presence of lattice planes which confirm the crystalline nature of the sample. The effect of La^{3+} ions on dielectric properties are presented in this paper.

Key words: *Nano ferrites, X-ray, IR and HRTEM*

Introduction:

Nanostructure materials are the promising candidates for variety of applications in recent technologies due their excellent electrical, optical, and magnetic properties that often show different behavior from their bulk counterparts.

The magnetic properties of nanomaterials are influenced by a number of factors such as: synthesis method, composition, particle size, shape, surface morphology, purity and interactions between particles.

Among magnetic materials, cobalt ferrite with spinel structure AB_2O_4 type is especially interesting owing to its magnetic properties such as strong anisotropy, high coercivity at room temperature and moderate saturation

magnetization, good mechanical and chemical stability [1]. Also, cobalt ferrites have low cost, high performance for high frequency applications.

Magnetic properties for cobalt ferrite can be modified promisingly by doping the rare earth elements. La^{3+} is a non-magnetic rare earth cation as it has not 4f electrons [2]. Its ionic size is much larger than the ionic size of Fe and Co ions. So, little amount solid solution of La^{3+} in CoFe_2O_4 may create lattice strain in the material and it leads to modify the magnetic structure. The magnetic properties can be modified due to change in magnetic structure.

From above discussion it is clear that cobalt ferrites are very useful and it is of interest to investigate the effect of rare earth ions on the properties of cobalt ferrites. Our interest is to modulate the properties of cobalt ferrites. The aim of the present work is to produce lanthanum doped cobalt ferrites which have high resistivity and are single phase for using in different applications.

Our work will be intended to synthesize nanoparticles with desired properties like magnetic moment, high permeability, resistivity, high dielectric constant, low dielectric loss.

Results and Discussions

1. X-ray Diffraction Analysis:

X-ray diffraction pattern (XRD) of CoFe_2O_4 samples doped with lanthanum with molar ratio 0.05, 0.1, 0.15, 0.2, 0.25 and 0.3, for samples prepared by auto consumption flash method were given in a previous work [3]. Flash samples are assigned by (f).

Cation distribution was estimated among the tetrahedral and octahedral interstitial sites. The estimated cation distribution is given in Table 1.

Small fraction of LaFeO_3 phase has been reported in La^{3+} doped spinel ferrite which is believed to be due to smaller solubility of La in such ferrite [4,5,6]. However the solubility limit of La^{3+} is yet to be investigated. The solubility normally depends on the conditions and method of synthesis of nano structure materials.

In our case the XRD analysis provide an evidence of LaFeO_3 phase at high concentration of La with $x=0.3$ in flash samples. This is in good agreement with the previous studies of La^{3+} doped spinel ferrite nano particles [7,8].

More doping concentration of La^{3+} leads to higher potential barrier for La^{3+} ion to overcome the entering into the spinel crystal lattice. This process leads to the formation of some foreign peaks as LaFe_2O_3 in addition to the spinel phase. So we conclude that the La^{3+} ion can be substituted for Fe^{3+} ion only when the samples are in nanocrystalline form have a large surface which leads to incorporate large ion (La^{3+}) in the lattice sites.

The analysis of the crystallite size has been carried out using the peak broadening and Scherer equation. The average crystallite size for consumption flash samples obtained by Scherer equation was about 22nm for CoFe_2O_4 and CoFe_2O_4 doped with La^{3+} . This value is coinciding with the average crystallite size of CoFe_2O_4 in literature [9].

It reveals that the substitution of La^{3+} in place of Fe^{3+} ion, a crystalline anisotropy due to large size mismatch of La^{3+} and Fe^{3+} , creates strain inside the volume of crystal which increases with increase of La^{3+} concentration. Therefore the present system remains in stable equilibrium by balancing crystal anisotropy and volume strain to each other.

In order to relax the volume strain, the crystalline size decreases with increasing La^{3+} concentration. After certain limit of La^{3+} the crystalline size increases again. This is because the formation of foreign phase after this limits which may affect the crystalline anisotropy [10].

La content	Cation distribution
$x=0.05$	$(\text{La}_{0.005}\text{Co}_{0.08}\text{Fe}_{0.95})[\text{La}_{0.045}\text{Co}_{0.92}\text{Fe}]$
$x=0.1$	$(\text{La}_{0.005}\text{Co}_{0.1}\text{Fe}_{0.9})[\text{La}_{0.095}\text{Co}_{0.9}\text{Fe}]$
$x=0.15$	$(\text{La}_{0.005}\text{Co}_{0.07}\text{Fe}_{0.85})[\text{La}_{0.145}\text{Co}_{0.93}\text{Fe}]$
$x=0.2$	$(\text{La}_{0.005}\text{Co}_{0.06}\text{Fe}_{0.8})[\text{La}_{0.195}\text{Co}_{0.94}\text{Fe}]$
$x=0.25$	$(\text{La}_{0.005}\text{Co}_{0.08}\text{Fe}_{0.75})[\text{La}_{0.245}\text{Co}_{0.92}\text{Fe}]$
$x=0.3$	$(\text{La}_{0.005}\text{Co}_{0.005}\text{Fe}_{0.7})[\text{La}_{0.295}\text{Co}_{0.995}\text{Fe}]$

Table (1) The cation distribution for the Co ferrite system doped with La.

One can observe that the concentration of La^{3+} ions is very low at the A site. Hence we conclude that the La^{3+} ions show a preference of octahedral site. From the occupancy variation we have observed that Co^{2+} ions occupy both tetrahedral and octahedral sites. Hence the present samples are in mixed spinel structure.

Radius of the octahedral site (R_B) is larger than the tetrahedral site (R_A) in the spinel lattice. The ionic radius of La^{3+} ions is larger enough for octahedral sites. One can assume that small amount of La^{3+} cations can be substituted for Fe^{3+} cations which enter into the octahedral site by rearrangement of cation between A and B

sites to minimize the free energy of the system. The variation of R_A and R_B are shown in Fig (1).

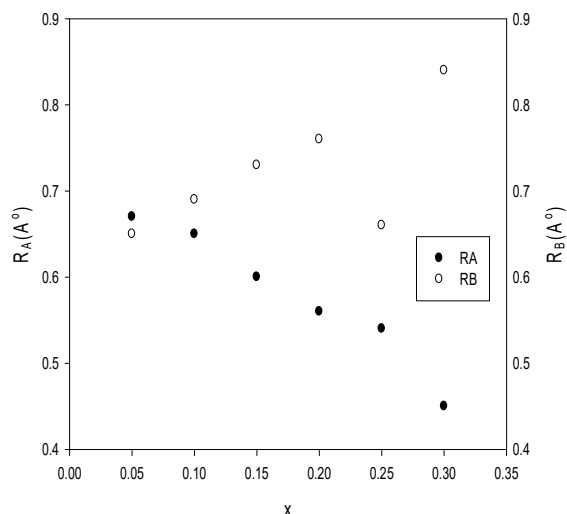


Fig (1) The radius of tetrahedral site (R_A) and the radius of octahedral site (R_B) vs. La content

Partial migration of Co^{2+} ions (0.74Å^0) from B to A sites has been observed by increasing La^{3+} concentration, accompanied by an opposite transfer of equivalent number of Fe^{3+} (0.64Å^0) from A to B sites in order to relax the strain at octahedral site. Hence the lattice constant decrease with increase of La^{3+} concentration.

2. IR studies:

FTIR spectra of the as prepared (f) samples sintered at 1200°C are shown in Fig 2. The absorption bands that occur at 3600cm^{-1} are corresponding to characteristic vibration of OH groups not associated with the hydrogen bond provided by citric acid.

The broad band is probably including bands in (f) samples corresponding to CH and CH_2 groups. The band located at 1628cm^{-1} is due to asymmetrical vibration of COO groups while the band from 1387 to 1435cm^{-1} corresponds to the symmetric vibration of the COO group [11]. The presents of these bands confirmed that the carboxyl groups are coordinated to the metal ions.

The intensity of the band situated at 1435 for (f) samples is splitting due to the overlapping of

symmetric vibration of carboxyl groups and asymmetric vibrations of the C-O-C groups.

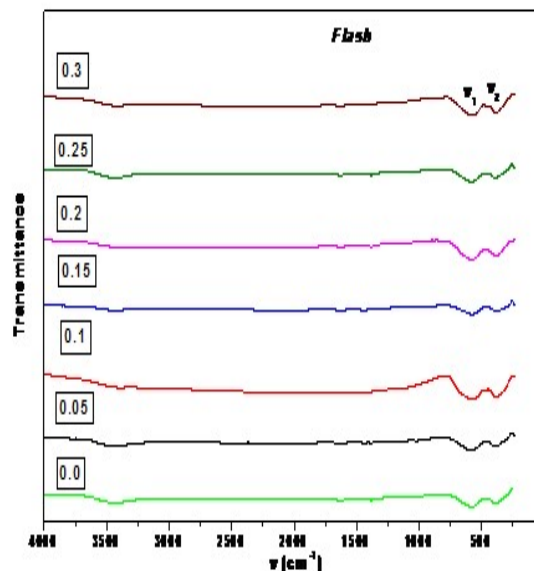


Fig (2) FTIR absorption spectra of Co ferrite doped with La for flash samples.

The FTIR spectroscopy is very useful technique to understand the molecular dynamics and usually assigned to the vibration of ion in the crystal lattice. The formation of spinel structure in the nanocrystal lattice and its cation distribution is supported by FTIR analysis. The FTIR spectra indicate the presence of absorption band in the range from 380 - 877cm^{-1} which is common feature of the spinel ferrite [12].

The higher frequency absorption band (ν_1) lies in the range of 572 - 580cm^{-1} for (f) samples. It is assigned to vibration of the tetrahedral metal complex which is the band between the oxygen ion and the tetrahedral metal ion ($M_{\text{tet}}\text{-O}$).

Lower frequency absorption band (ν_2) lies in the range 400 - 490cm^{-1} and it is assigned to vibration of octahedral metal complex which is bond between the O^{2-} ion and the octahedral metal ion ($M_{\text{oct}}\text{-O}$) [13]. This band position is found to be in agreement with the characteristic infrared absorption band of CoFe_2O_4 nanocrystal [14,10]. The peak positions of the absorption bands changes with the doping of La^{3+} ion in place of Fe^{3+} ions. The change in the band positions is due to the change in ($M_{\text{tet}}\text{-O}$) and ($M_{\text{oct}}\text{-O}$) bond lengths [15].

The difference between the tetrahedral and octahedral frequency bands is due to the change in bond length of M-O at octahedral and tetrahedral sites. The two weak and broad absorptions around 1400 to 1600 cm^{-1} corresponding to the presence of small amount of residual carbons in the (f) samples, indicating that the residual carbon has mostly burnt away during the self combustion process.

Small peaks at 1019 to 1100 cm^{-1} may be due to carbonate group [16], which is still present in the sample in stable and need 1400 $^{\circ}$ C to be eliminated from the sample. Traces of nitrate ion are also detected by the appearance of peak at 1400 cm^{-1} . The metal oxide bands for octahedral and tetrahedral become stronger as the La^{3+} content increase [17].

Since the frequency is proportional to the force constant, the calculated values of force constant for both tetrahedral and octahedral sites are given in Table (2) from the following equation [18]:

$$F=4\pi^2c^2U^2m$$

Where C is the velocity of light in (cm/sec), U is the wave number and m is the reduced mass equals $\frac{m_1m_2}{m_1+m_2}$. The force constant of tetrahedral and octahedral sites increases then decreases.

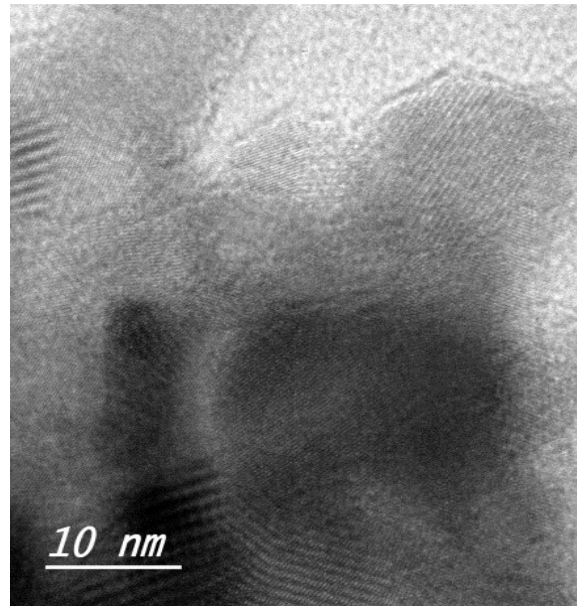
X	Flash	
	F_{tetra}	F_{octa}
0.05	$24 \cdot 10^4$	$10 \cdot 10^4$
0.1	$24 \cdot 10^4$	$10 \cdot 10^4$
0.15	$24 \cdot 10^4$	$10 \cdot 10^4$
0.2	$24 \cdot 10^4$	$10 \cdot 10^4$
0.25	$24 \cdot 10^4$	$10 \cdot 10^4$
0.3	$24 \cdot 10^4$	$10 \cdot 10^4$

Table (2) The force constant of tetrahedral site (F_{tetra}) and octahedral site (F_{octa}) for the Co ferrite system doped with La.

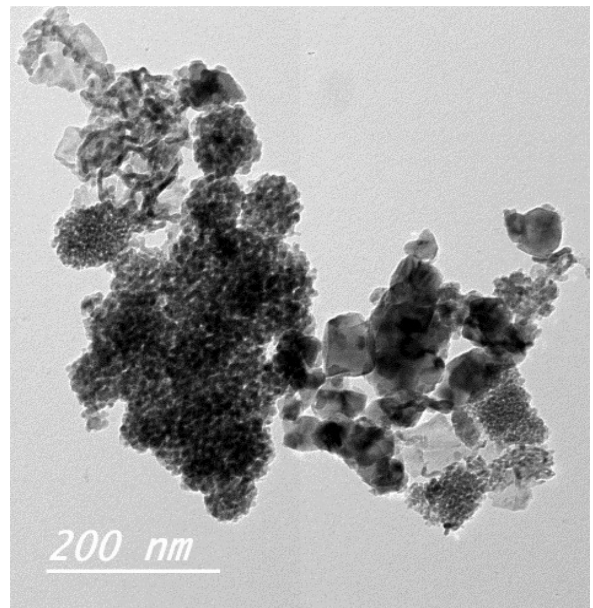
3- HRTEM:

Fig (3) show the HRTEM image of CoFe_2O_4 nanoparticles prepared by (f) method for samples $x=0.05, 0.15$ and 0.25 . The image

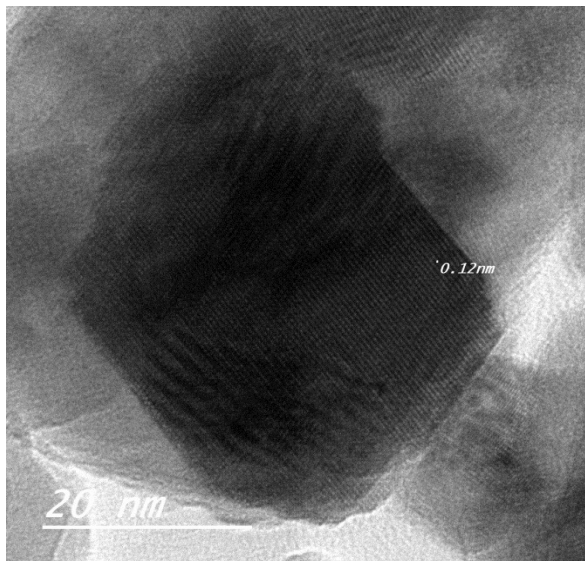
clearly shows the presence of cubic nanoparticles with average diameter of 16nm.



$x=0.05(f)$



$x=0.15 (f)$



x=0.25 (f)

Fig(3) HRTEM images of $\text{La}_x\text{CoFe}_{2-x}\text{O}_4$ for x=0.05, 0.15 and 0.25 of (f) samples.

The particle size obtained from HRTEM micrograph is lower than that obtained from XRD which was 22nm which may be due to the agglomeration of some particles. It is shown from the micrographs that there are no isolated particles which reveals that there are a lot of small particles conglomerated together to form a larger particle in the powders. This agglomeration shows that the particles are attracted toward each other indicating their magnetic character [19].

The results of crystallite size confirming the formation of nanoparticle. The analysis of TEM image shows that there is a change in structure of CoFe_2O_4 after La^{3+} doping. The agglomeration makes the individual identification of the crystallite difficult; also in x-ray the presents of multi phases affect the line broadening results in different particle size. These reasons cause in consistent between the results obtained from HRTEM and XRD.

The increase in particle size with La^{3+} doping is evident from HRTEM. Most of nanoparticles are agglomerates due to the tendency of nanoparticle to achieve a low free energy state by reducing the specific superficial area with other particle [20]. The average particle size calculated from HRTEM images are given in

Table3. Values are most comparable with the crystallite size obtained by XRD.

X	Average size (nm)	
	Flash	
	XRD	TEM
0.05	21.72	14.27
0.15	17.83	6.38
0.25	18.23	16.98

Table (3) The particle size determined from HRTEM and XRD.

The HRTEM images for four samples have lattice spacing which confirms the crystalline nature of the samples. The inter planer distance obtained from HRTEM for $\text{La}_{0.15}\text{CoFe}_{1.85}\text{O}_4$ was found to be 0.09nm which coincide with the plane (062) given from XRD pattern. The HRTEM for other samples gives d-spacing 0.19nm for the sample x=0.05(f), 0.14nm for the sample x=0.15(f) and 0.12nm for x=0.25(f) which are coincide with the planes (004), (313) and (421) respectively which are given in Table4.

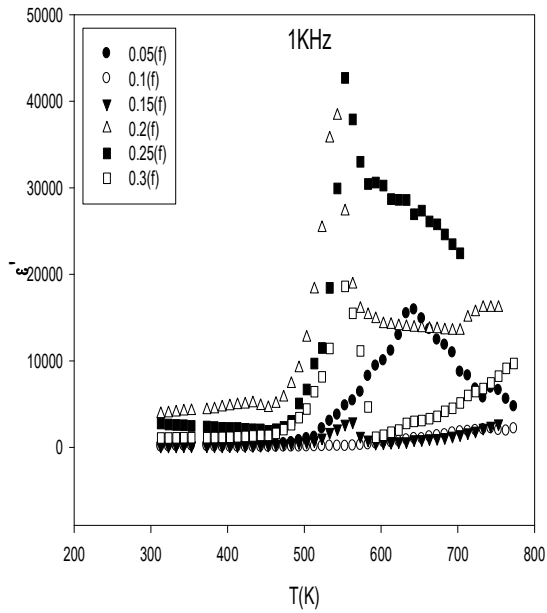
X	d-space(nm)	
	XRD	TEM
0.05	0.193	0.19
0.15	0.143	0.14
0.25	0.120	0.12

Table (4) The d-space determined from HRTEM and XRD.

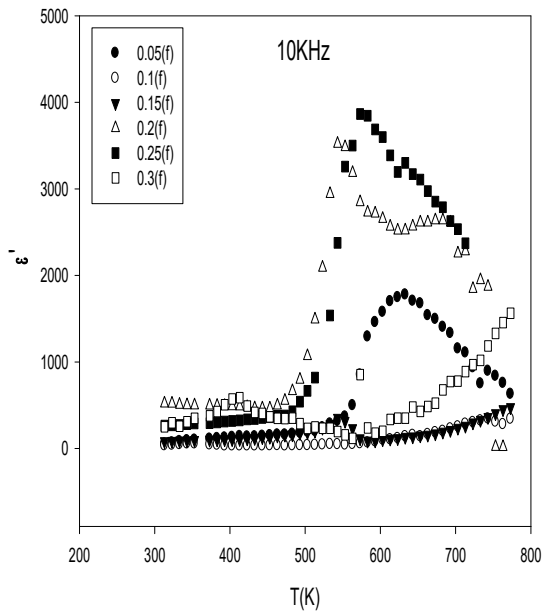
3. Electrical properties

3.1. Dielectric constant

The effect of temperature on dielectric constant of the composition $\text{La}_x\text{CoFe}_{2-x}\text{O}_4$ at 1 and 10KHz in temperature region from room temperature to 800K is illustrated in Fig 4 (a,b).



(a)



(b)

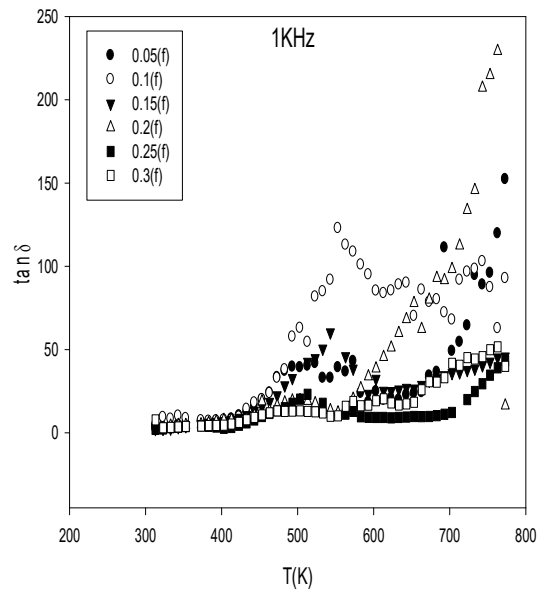
Fig 4 (a,b): The dielectric constant as a function of temperature for flash samples.

The dielectric constant increases gradually with increasing temperature up to particular temperature which is designated as dielectric

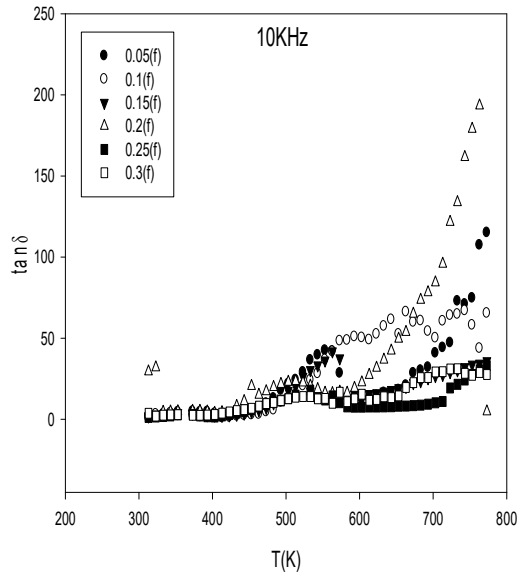
transition temperature (Curie temperature). A similar temperature variation of dielectric constant has been reported earlier [21,22]. The non zero value of the dielectric constant at high temperature increases with La concentration. This provides strong evidence for the existence of Debye relaxation process [23]. It has been observed in many cases that the conduction and dielectric mechanism in ferrites are similar according to Rezlescu model [24].

3.2. Dielectric loss

Fig 5 (a,b) shows the variation of dielectric loss with temperature and frequency. The dielectric loss increases gradually with temperature up to 500K. The dielectric loss ($\tan\delta$) decreases by increasing frequency. The decrease in dielectric loss with increasing frequency is according to Koops phenomenological model [25]. The peak occurs around 700K when the frequency of the applied field is equal to the hopping frequency [26].



(a)



(b)

Fig 5 (a,b): The dielectric constant as a function of temperature for flash samples.

Generally decrease in dielectric loss is attributed to the decrease in polarization of the sample as the dipole cannot follow up the field variation [27]. The decrease in dielectric loss ($\tan\delta$) with frequency takes place when the hopping rate of electrons lags behind the alternating electric field beyond a certain critical frequency. The dielectric loss is an important part for low core loss in ferrite [28]. Hence for low core loss, low dielectric loss is desirable.

Conclusion

$\text{La}_x\text{CoFe}_{2-x}\text{O}_4$, where $x=0.05, 0.1, 0.15, 0.2, 0.25, 0.3$ were prepared by flash method and their electrical properties and the crystalline phases have been compared.

The X-ray diffraction patterns for $\text{La}_x\text{CoFe}_{2-x}\text{O}_4$ showed that the pattern has single phase crystalline structure with no impurity peaks present in the pattern which confirm that La^{3+} , Fe^{3+} have been incorporated into spinel lattice. The average crystallite size for consumption flash samples obtained by Scherer equation was

about 22nm for CoFe_2O_4 and CoFe_2O_4 doped with La^{3+} .

The FTIR confirms the formation of spinel structure. The bond length of $\text{Fe}^{3+}-\text{O}^{2-}$ was calculated and was correlated with the variation of ν_1 and ν_2 .

The HRTEM image of CoFe_2O_4 shows the presence of cubic nanoparticles with average diameter of 16nm. It is shown from the micrographs that there are no isolated particles which prefer to be in groups and agglomerates of many particles are clearly seen. The inter planer distance obtained from HRTEM for $\text{La}_{0.15}\text{CoFe}_{1.85}\text{O}_4$ was found to be 0.09nm which coincide with the plane (062) given from XRD pattern.

Dielectric constant and dielectric loss increase gradually with increasing temperature up to particular temperature which is designated as dielectric transition temperature (Curie temperature) and they decrease by increasing frequency.

References

- 1) J.G. Lee, J.Y. Park, Y.J. Oh, C.S. Kim, Magnetic properties of CoFe_2O_4 thin films prepared by a sol-gel method, *J. Appl. Phys.*, 84, 2801-2804, (1998).
- 2) R. Valenzuela, *Magnetic Ceramics*, Cambridge University Press, 1994.
- 3) S.F. Mansour, O.M. Hemeda, S.I. El-Dek, B.I. Salem. *Journal of magnetism and magnetic materials*, 420 (2016) 7-18.
- 4) Atta ur Rahman, M.A. Rafiq, S.Karim, K. Mazz, M. Siddique, M.M. Hasan, *Physica B*, 406, 4393-4399, (2011).
- 5) P.K. Roy, Nayak B. Bibhuti, J. Bera, *J. Magn. Mater.* 320 (2008) 1128.
- 6) P.K. Roy, J. Bera, *Mater. Res. Bull.* 42 (2007) 77.
- 7) Pawan Kumara, S.K. Sharma, M. Knobel, M. Singh, *J. Alloys Compd.* 508 (2010)115.
- 8) Gu Ying-ying, Ta Xiao-ping, Lian Shu-Quan, Sang Shan-Bing, *J. Cent. South Univ. Technol.* 11 (2004) 166.
- 9) T. Minami, H. Sato, K. Ohashi, T. Tomofuji, S. Takata, *Conduction*

- mechanism of highly conductive and transparent zinc oxide thin films prepared by magnetron sputtering, *J. Cryst. Growth*, 117, 370-374, (1992).
- 10) Lawrence Kumar, Manoranjan Kar, *Ceramics International* 38, 4771-4782, (2012).
 - 11) X.F. Chu, D.L. Jiang, Y. Guo, C.M. Zheng, Ethanol gas sensor based CoFe_2O_4 nanocrystallines prepared by hydrothermal method, *Sens. Actuators B*, 120, 177-181, (2006).
 - 12) R.D. Waldron, *Infrared spectra of ferrites*, *Phys. Rev.* 99 (1955) 1727.
 - 13) C.G. Ramankutty, S. Sugunam, Surface properties and catalytic activity of ferros spinels of nickel, cobalt and copper prepared by soft chemical method, *Appl. Catal. A* 39 (2001) 128.
 - 14) S. Rana, J. Philip, B. Raj, Micelle based synthesis of cobalt ferrite nanoparticles and its characterization using Fourier transform infrared transmission spectroscopy and thermogravimetry, *Mater. Chem. Phys.* 124 (2010) 264-269.
 - 15) R.C. Kamble, K.M. Song, Y.S. Koo, N. Hur, Low temperature synthesis of nanocrystalline Dy^{3+} doped cobalt ferrite: structural and magnetic properties, *J. Appl. Phys.* 110 (2011) 053910.
 - 16) Nayak Himansulal, *Res. J. Material Sci.*, Vol. 3(2), 1-8, June (2015).
 - 17) NAFISAH OSMAN, NAJWA 'ADNI IBARAHIM, MOHD AZLAN MOHD ISHAK & OSKAR HASDINOR HASSAN, *Sains Malaysiana* 43(9)(2014): 1373–1378.
 - 18) O.M. Hemeda, M.M. Barakat and D.M. Hemeda, *Turk J Phys.* 27, (2003) 537.
 - 19) P. Kumar, J. Chand, Satish Verma, M. Singh, *International Journal of Theoretical and Applied Science* 3(2): 10-12(2011).
 - 20) S. Da Dalt, A.S. Takimi, T.M. Volkmer, V.C. Sousa, C.P. S. Da Dalt, A.S. Takimi, T.M. Volkmer, V.C. Sousa, C.P. Bergmann, Magnetic and Mossbauer behavior of the nanostructured MgFe_2O_4 spinel obtained at low temperature, *Powder technology* 210 (2011)103-108.
 - 21) E. Ranga Mohan, D. Ravinder, A. V. Ramana Reddy, B. S. Boyamov, *Mat. Lett.* 40, (1999), 39-45.
 - 22) S. A. Olofa, *J. Magn. Magn.* 131, (1994), 103.
 - 23) M.H Abdullah, A.N Yusoff, *J. Mat. Science* 32 (1997) 5817.
 - 24) N. Rezlescu, *Phys. Status Solidi* 23 (1974) 575.
 - 25) C.G. Koops, *Phys. Rev.* 83 (1951) 121.
 - 26) A.S. Hudson, *Marconi Rev.* 37 (1978) 43.
 - 27) Rakesh Kr Singh, Amarendra Narayan, Structural, Magnetic & Dielectric behavior of $\text{Ni}_{0.5}\text{Zn}_{0.5}\text{Fe}_{1.99}\text{R}_{0.01}\text{O}_4$ Nanoparticles; R= Pr, Sm and Gd, synthesized using Citrate Precursor method, annealed at low temperature 450C, *International Journal of Engineering and Technical Research (IJETR)*, ISSN: 2321-0869, Volume-2, Issue-8, August 2014.
 - 28) J. Zhu, K.J. Tseng, C.F. Foo, *IEEE Trans. Magn.* 36 (2000) 3408.

بسنت ابراهيم سالم

قسم الفيزياء- كلية العلوم- جامعة طنطا

يهدف هذا البحث الي دراسة الخواص الكهربائية لمركب نانو فريتى ذا التركيب الكيميائي التالي: $La_xCoFe_{2-x}O_4$ بنسب $x=0.05, 0.1, 0.15, 0.2, 0.25, 0.3$

وتم تحضير هذه العينات بطريقة الفلاش وتمت دراسة خواص المركب باستخدام حيود الأشعة السينية ودراسة طيف المتصاص للأشعة تحت الحمراء والميكروسكوب الإلكتروني. وقد دلت دراسة حيود الأشعة السينية للعينات علي أن التركيب البلوري مكعب الشكل دون وجود غيره من الأطوار الأخرى والأكاسيد. وأكدت دراسة طيف الامتصاص للمركبات باستخدام مطياف الأشعة تحت الحمراء وجود الشبكتين لفريتات $La_xCoFe_{2-x}O_4$ وهذا ما أظهرته دراسة حيود الأشعة السينية. وبينت أطياف الأشعة تحت الحمراء وجود حزمتي امتصاص عند الترددات المتوقعة كما تم تحديد تردد الاهتزاز للروابط $Fe^{3+}-O^{2-}$ في الشبكة الفرعية ذات التردد الرباعي والثماني. كما أظهرت نتائج استخدام الميكروسكوب الإلكتروني وجود التركيب البلوري المكعب الشكل بمتوسط قطر 16 نانومتر. وتم أيضا حساب حجم الحبيبات عن طريق استخدام المسح الإلكتروني للعينات. تم أيضا حساب ثابت العزل وثابت الفقد الكهربى ووجد انهم يزدادوا بزيادة درجة الحرارة.